NeuroImage: Clinical 12 (2016) 451–459

Contents lists available at ScienceDirect

NeuroImage: Clinical

journal homepage: www.elsevier.com/locate/ynicl

Resting-state fMRI study of acute migraine treatment with kinetic oscillation stimulation in nasal cavity

Tie-Qiang Li[a,b,*], Yanlu Wang[b], Rolf Hallin[c], Jan-Erik Juto[b]

[a]Department of Medical Physics, Karolinska University Hospital Huddinge, Sweden
[b]Department of Clinical Science, Intervention and Technology, Karolinska Institute, Stockholm, Sweden
[c]Department of Physiology and Pharmacology, Division of Clinical Neurophysiology, Karolinska University Hospital, Huddinge, Sweden

ARTICLE INFO

Article history:
Received 30 November 2015
Received in revised form 22 July 2016
Accepted 13 August 2016
Available online 15 August 2016

Keywords:
Kinetic oscillatory stimulation (KOS)
Migraine
Autonomic nervous system (ANS)
Resting-state fMRI
Intrinsic functional activity
Independent component analysis (ICA)
3-Way ANOVA

ABSTRACT

Kinetic oscillatory stimulation (KOS) in the nasal cavity is a non-invasive cranial nerve stimulation method with promising efficacy for acute migraine and other inflammatory disorders. For a better understanding of the underlying neurophysiological mechanisms of KOS treatment, we conducted a resting-state functional magnetic resonance imaging (fMRI) study of 10 acute migraine patients and 10 normal control subjects during KOS treatment in a 3 T clinical MRI scanner. The fMRI data were first processed using a group independent component analysis (ICA) method and then further analyzed with a voxel-wise 3-way ANOVA modeling and region of interest (ROI) of functional connectivity metrics.

All migraine participants were relieved from their acute migraine symptoms after 10–20 min KOS treatment and remained migraine free for 3–6 months. The resting-state fMRI result indicates that migraine patients have altered intrinsic functional activity in the anterior cingulate, inferior frontal gyrus and middle/superior temporal gyrus. KOS treatment gave rise to up-regulated intrinsic functional activity for migraine patients in a number of brain regions involving the limbic and primary sensory systems, while down regulating temporally the activity for normal controls in a few brain areas, such as the right dorsal posterior insula and inferior frontal gyrus.

The result of this study confirms the efficacy of KOS treatment for relieving acute migraine symptoms and reducing attack frequency. Resting-state fMRI measurements demonstrate that migraine is associated with aberrant intrinsic functional activity in the limbic and primary sensory systems. KOS in the nasal cavity gives rise to the adjustment of the intrinsic functional activity in the limbic and primary sensory networks and restores the physiological homeostasis in the autonomic nervous system.

© 2016 Published by Elsevier Inc. This is an open access article under the CC BY-NC-ND license (http://creativecommons.org/licenses/by-nc-nd/4.0/).

1. Introduction

Migraine is a common, neurological disorder characterized by severe headache and affecting approximately 18% of women and 6% of men (Friedman and De ver Dye, 2009; Scher et al., 2005; Schwedt et al., 2015). Triptans such as sumatriptan are widely used for acute symptom relief of migraine headaches. About 2% of the population suffers from refractory chronic migraine and the trigeminal autonomic cephalalgias (TACs), which is often associated with drug-resistance, disability and low quality of life.

There exist a number of theories trying to account for the ethnology of migraine. For example, inadequate regulation of the autonomic nervous system (ANS) (Ebinger et al., 2006; Geraud and Donnet, 2013; Melek et al., 2007), derangement of serotonin metabolism (Dussor, 2014; Hoffmann and Goadsby, 2014; Vollbracht and Rapoport, 2014), insensitive reaction to reduced oxygen in the vasculature and tissue (Friberg et al., 1994; Lacombe et al., 1992; Raddant and Russo, 2014), disruption of the normal pain pathways (Kroger and May, 2015), peculiar platelet metabolism (Danese et al., 2014; Gawel and Rose, 1982; Hanington, 1989), neurogenic inflammation (Tajti et al., 2015) and etc. (Alstadhaug, 2014). Researchers have yet to disseminate a unified theory to account for the different aspects of the complex pathophysiology of migraine. Despite extensive neuroimaging studies of headache disorders in the last decade (Arkink et al., 2012; Charles, 2013; Kroger and May, 2014; Lipton et al., 2014; Maniyar et al., 2014; Maniyar et al., 2015; May, 2013; Montagna et al., 2010; Morelli et al., 2013; Moulton et al., 2014; Robert et al., 2013; Sahler, 2013; Schwedt et al., 2015; Seifert et al., 2012; Zielman et al., 2014), functional imaging acquired during transient attack of migraine has been quite rare. Such studies can provide important insight into the pathogenesis of migraine headaches. Earlier PET studies have shown persisting activation in the brain stem and hypothalamus during migraine attacks (Bahra et al., 2001; Geraud et al., 2005). MRI studies based on arterial spin labeling (ASL) have also reported hemodynamic abnormality in the

* Corresponding author at: Department of Medical Physics, Karolinska University Hospital Huddinge, 141 86 Stockholm, Sweden.
E-mail address: tie-qiang.li@karolinska.se (T.-Q. Li).

http://dx.doi.org/10.1016/j.nicl.2016.08.014
2213-1582/© 2016 Published by Elsevier Inc. This is an open access article under the CC BY-NC-ND license (http://creativecommons.org/licenses/by-nc-nd/4.0/).

hypothalamus during treatment of migraine with triptan (Arkink et al., 2012; Kato et al., 2010; Pollock et al., 2008). These findings have led to the hypothesis that hypothalamic pathway might play a critical role in the pathogenesis of migraine attacks (Moulton et al., 2014; Robert et al., 2013; Schwedt et al., 2015). Results from neuroimaging and spectroscopy studies of TACs provided further evidence for this view (Iacovelli et al., 2012; Lodi et al., 2006; Wang et al., 2006). For TACs and refractory migraine, hypothalamic deep brain stimulation has been tested as an alternative treatment and symptom reduction has been observed in some patients (Altinay et al., 2015; Palmisani et al., 2013).

Taking advantages of the rich innervations and inter-nerve connections in the nasal mucous membrane, we have recently developed a non-invasive approach based on kinetic oscillatory stimulation (KOS) in the nasal cavity for the treatment of migraine (Juto and Hallin, 2015) and other chronic inflammatory disorders (Juto and Axelsson, 2014). We have completed a randomized control trial (RCT) study (ClinicalTrials.gov Identifier: NCT01488110) based on 36 migraine patients and showed that KOS in the nasal cavity is an effective and safe method to relieve both acute pain and reduce the attack frequency in patients with migraine (Juto and Hallin, 2015). Multi-site clinical RCT studies for further testing its efficacy on acute migraine (ClinicalTrials.gov Identifier: NCT02185703) and prophylactic effects (ClinicalTrials.gov Identifier: NCT02243865) are currently under way.

The purpose of this study is to improve our understanding of the neurological underpinnings for KOS treatment of acute migraine. Such understanding may provide guidance for further optimization of the procedure and extension of KOS method for other clinical applications in addition to the treatment of migraine. We used blood oxygen-level dependent (BOLD) functional magnetic resonance imaging (fMRI) technique to study the alterations in the functional connectivity in the brain in response to the KOS treatment. We compare the resting-state functional connectivity differences between patients with acute migraine and normal volunteers before, during and after KOS treatment. We demonstrate that migraine headache is associated with abnormal intrinsic functional connectivity in the limbic system, which is the central brain network for ANS control and KOS treatment can regulate the functional connectivity of the limbic system back to normal status.

2. Materials and methods

2.1. Recruitment and clinical evaluation of the migraine patients

We recruited 10 adult patients (male/female = 5/5, age = 44 ± 10) and 10 normal controls (male/female = 5/5, age = 43 ± 11) into the study. The patients were previously diagnosed with migraine according to the ICHD-2 classification and experienced at least one migraine attack per month before participating in the study. The migraine patients had no other significant disease. The patients contacted the investigators by phone at typical signs of an attack development. Their headache had to fulfill the ICHD-2 criteria and reach at least 4.0 on the pain visual analog scale (VAS) 0–10. VAS = 0 presents no pain and VAS = 10 the highest level of unbearable pain. We administered the actual KOS treatment inside a clinical MRI scanner within 30 min of arrival on site. Patients were asked not to take any medication before the KOS treatment (see Table 1) (Li et al., 2014, 2015b).

The VAS assessment of pain was conducted immediately before the KOS treatment, every 10 min during treatment, at the end of the treatment and 15 min after treatment. All patients were also asked to assess their general well-being immediately before and following the treatment. The pain level was also assessed 24 h after by telephone interview. After the KOS treatment the patients were requested to continue with their VAS assessment of pain and report to the investigators. In case of migraine reoccurrence, we provided the patients with the option of repeated KOS treatments.

Table 1
Summary of the clinical information for the 10 migraine patients.

Patient	Sex	Age	Pain	Pain free period	KOS repetition
1	f	40	7	6 months	2
2	m	37	6	3 months	1
3	m	43	7	3 months	1
4	f	35	8	6 months	4
5	f	41	5	5 months	1
6	f	53	6	6 months	2
7	m	61	8	5 months	3
8	m	61	4	3 months	2
9	m	42	5	3 months	2
10	f	31	4	3 months	2

2.2. KOS treatment

KOS in the nasal cavity was administered using the similar equipment described in our previous studies (Juto and Axelsson, 2014; Juto and Hallin, 2015; Li et al., 2014, 2015b). It consists of a controller unit connected to a single-use catheter through a 7 m long plastic tube, which can deliver oscillatory stimulations to the nasal mucosa, while the patients were positioned inside the MRI scanner for fMRI measurements. The catheter coated with lubricating liquid (medical grade paraffin or water) was inserted into the nasal cavity on the side with the predominant pain. We chose to treat the right side first, if the patients had no lateralization with their symptoms. For active treatment of migraine, the tip was inflated and oscillated for 10 min at the pressure of 95 mbar and frequency of 68 Hz. After 10 min the oscillations were terminated and the patients were asked to assess their pain level. In case of some remaining pains, the catheter was deflated and moved to the other side, re-inflated and the treatment continued for another 10 min.

It should be noted that the device can deliver KOS inside the entire nasal cavity, extending deep in the proximity of the pterygopalatina ganglion (PPG). The settings (pressure and frequency) and treatment duration are based on previous clinical experience (Juto and Axelsson, 2014; Juto and Hallin, 2015) and are usually optimized for each specific disorder and patient sub-groups. For example, the optimal settings for the treatment of non-allergic rhinitis were 50 mbar and 50 Hz (Juto and Axelsson, 2014), whereas 95 mbar and 68 Hz are more effective for acute migraine (Juto and Hallin, 2015; Li et al., 2014, 2015b).

2.3. fMRI data acquisition

The fMRI measurements were conducted using a 3 T whole-body clinical MRI scanner (TIM Trio, Siemens Healthcare, Erlangen, Germany). A single-shot 2D gradient-recalled echo echo-planar imaging pulse sequence was used for the data acquisition with the following main acquisition parameters: 32 transverse slices, slice thickness = 3.6 mm, TR/TE = 2000/35 ms, FOV = 220 mm, matrix size = 64 × 64, flip angle = 90°, 300 dynamic timeframes, and IPAT = 2. A 32-channel phased-array head coil was used for the signal reception. Foam padding was used to for each subject to reduce involuntary head motions.

For each migraine subject we conducted 4–5 sessions of BOLD fMRI scans lasting 10 min per session. The migraine headache was on going at the time of arrival for fMRI. Prior to the active KOS treatment, we performed two control resting-state fMRI scans for each patient. A baseline measurement session without inserted probe (denoted as Base1) and another session with inserted catheter but no active oscillatory stimulations (denoted as Probe). Depending on the symptom assessment if the migraine pain diminished completely after one session, we administrated one or two sessions of active KOS treatment for each patient inside the MRI scanner while continuous BOLD fMRI recording was also carried out (denoted as KOS). However, to facilitate comparison only the data acquired during KOS treatment of the right nasal cavity entered into the analysis. At the end, we performed also a post-treatment control

session of resting-state fMRI scan (Base2) after removing the KOS catheter.

Since KOS in nasal cavity is a non-invasive treatment, for comparison we applied the same treatment procedure and fMRI protocol described above to the normal controls. The active KOS treatment was administrated on both sides with the order of right to left.

2.4. fMRI data pre-processing

The resting-state fMRI datasets underwent a pipeline of preprocessing procedure, which were performed with AFNI (http://afni.nimh.nih.gov/afni) and FSL (http://www.fmrib.ox.ac.uk/fsl) programs with a bash wrapper shell(Wang and Li, 2013, 2015). The first 10 timeframes in each data set were removed to ensure signal steady state. After temporal de-spiking, six-parameter rigid body image registration was performed for motion correction. The average volume for each motion-corrected time series was used to generate a brain mask to minimize the inclusion of the extra-cerebral tissues. Spatial normalization to the standard MNI template was performed using a 12-parameter affine transformation and mutual-information cost function. During the affine transformation the imaging data were also re-sampled to isotropic resolution using a Gaussian kernel with 4 mm full width at half maximum (FWHM). Nuisance signal removal was achieved by voxel-wise regression using 16 regressors based on the motion correction parameters, average signal of the ventricles, average signal of the core white matter and their 1st order derivatives. After baseline trend removal up to the third order polynomial, effective band-pass filtering was performed using low-pass filtering at 0.08 Hz. At last local Gaussian smoothing up to FWHM = 6 mm was performed using an eroded gray matter mask.

2.5. Group ICA and statistical assessment

To create group level functional connectivity network parcellation we performed ICA on the pre-processed resting-state fMRI data using the GIFT toolbox (mialab.mrn.org/software) implemented in MATLAB (MathWorks, Massachusetts, USA). It included a series of analytical steps similar to the standard group ICA procedure (Wang and Li, 2013, 2015). Individual datasets were first concatenated and then followed by computation of the individual ICA components and corresponding time courses. Data reduction based on principle component analysis was performed at the subject and group levels prior to ICA. The Infomax algorithm was then applied to estimate the aggregate independent components (ICs). Lastly, subject specific spatial maps and time courses were estimated using the direct group ICA back-reconstruction approach. To prepare the subject specific ICA results for higher-level statistical assessment, the subject specific ICA results were rescaled with z-transformation.

To investigate how the specified number of independent components (NIC) influences ICA results, we performed group ICA of the pooled resting-state fMRI data with NIC systematically incremented from 2 to 19. We manually inspected the spatial distributions of the one-sampled *t*-test results of all ICs and the corresponding time courses to exclude possible artifacts. All non-artifacts ICs are considered as potential resting-state functional networks (RFNs). Mask was created for each potential RFN by imposing a voxel-wise t-score threshold of $t \geq 4.0$ ($p \geq 0.0008$, uncorrected) and a minimum cluster size $S \geq 20$. This guarantees a family-wise error rate (FWER) $p \leq 0.01$, as estimated by using the AFNI program, *AlphaSim +* with following inputs: voxel-wise $p < 0.0008$, FWHM = 6.2 mm, and 10^6 iterations. FWHM = 6.2 mm was the estimated average by applying the AFNI program, *3dFWHMx*, to the final smoothed fMRI data, which was quite close to FWHM = 6 mm used in the final smoothing procedure described above.

2.6. Statistics

We performed voxel-wise 3-way analysis of variance (ANOVA) of the ICA results to assess the functional connectivity differences between migraine patients and normal controls measured before, during and after the KOS treatment. We used the AFNI program, *3dANOVA3* with the model option of type = 5. In the model there are two fixed factors. One is the group difference between migraine patients and normal controls (degree of freedom, DF = 1) and the other is the KOS treatment effect occurred in the four scanning sessions: Base1, Probe, KOS, and Base2 (DF = 3). The participants in each group were modeled as a random factor (DF = 9). With the 3-way ANOVA, we can also assess the interaction between the two fixed factors and interrogate how the KOS treatment affected differently the intrinsic functional activity in migraine patients and healthy volunteers. We performed voxel-wise 3-way ANOVA for each RFN and only voxels within the RFN mask are considered.

The statistical significance of the 3-way ANOVA result for a given RFN was assessed first by setting an uncorrected voxel-wise threshold at $p \leq 0.01$ and then by imposing a minimum voxel cluster size of at least 20 contiguous voxels. The probability of random field of noise producing a cluster of size ≥ 20 was estimated at $p \leq 0.05$. This was concluded from the Monte-Carlo simulation result obtained by using the AFNI program, *AlphaSim +*. For the simulations we used following input parameters: voxel-wise threshold value $p \leq 0.01$, 10^6 iterations, the brain mask and FWHM = 6.2 mm. The final result for a given NIC is summarized as the non-zero mean of the ANOVA results for all potential RFNs.

2.7. ROI analysis of the brain functional connectivity metrics

To investigate the effect of the actual KOS treatment versus probe insertion we evaluated the brain functional connectivity for the ROIs which exhibit significant interaction between subject group and KOS treatment. We used a quantitative data-driven (QDA) approach to derive two metrics for quantifying the brain functional connectivity changes. The QDA approach has been described by us in details elsewhere (Nordin et al., 2016). In brief, the procedures used here are the following: Firstly, we compute the voxel-wise cross-correlation coefficient (CC) matrix. That is for each voxel inside the brain, we compute the Pearson's cross-correlation coefficients of the r-fMRI time course with that of every other voxel inside the brain. Secondly, we derive two voxel-wise metrics from the CC matrix, which are the connection strength index (CSI) defined as the non-zero mean value of the Pearson's cross-correlation coefficients ≥ 0.3 for all voxel pairs involving the current voxel in question and the connection counter index (CCI) defined as the number of voxel pairs involving the current voxel in question with the Pearson's cross-correlation coefficients ≥ 0.3. Lastly, we calculate the CCI and CSI average values for the ROI masks derived from the 3-way ANOVA.

3. Results

As summarized in Table 1, all migraine patients were fully relieved from their acute headache symptoms after 10–20 min KOS treatment inside the MRI scanner, which confirms the result from previous RCT study conducted outside the MRI scanner (Juto and Hallin, 2015). Furthermore, the patients experienced a prolonged period up to 3–6 months without migraine attacks, as assessed by telephone interviews after the fMRI study.

Figs. 1–3 depict the one-sampled t-score maps of the group ICA results (FWER $p \leq 0.01$) for NIC = 2–4, respectively. ICA parcellation with low NIC produced over-determined and functionally less specific networks. With increasing NIC, the detected RFNs become more functional specific. E.g. at the minimum NIC = 2, we observed the primary sensory network consisting of the somatosensory motor, auditory and visual systems (Fig. 1a) and the extended default mode network (Fig.

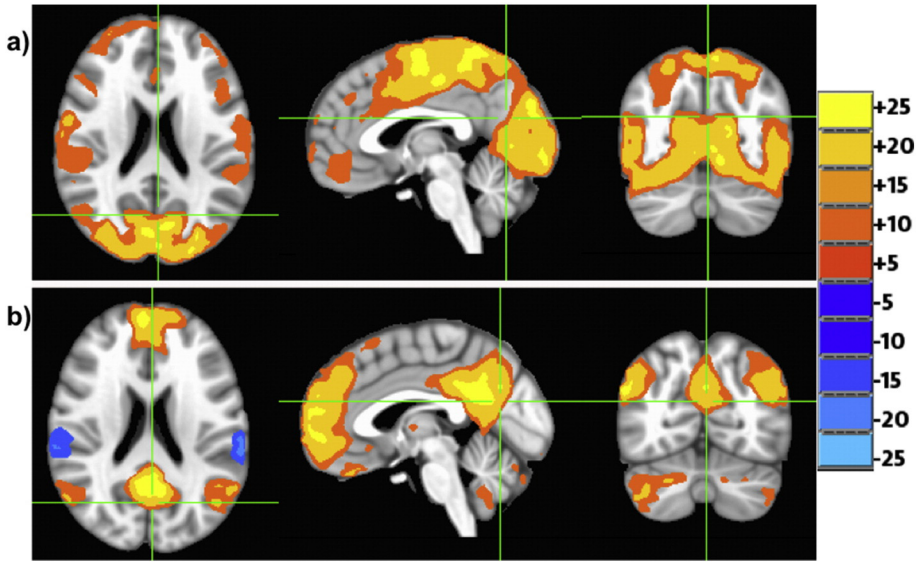

Fig. 1. The cross-sectional displays of the one-sampled t-score maps (t ≥ 4.0 and minimum cluster size of 20) for group ICA result at NIC = 2. (a) The somatosensory motor network in combination with the auditory and visual systems. (b) The extended default mode network. The color bar indicates the t-score level. (For interpretation of the references to color in this figure legend, the reader is referred to the web version of this article.)

1b). With NIC = 3, we observed an additional network (Fig. 2c) consisting of several left-right mirrored frontoparietal areas and corresponding to the combination of the left and right control networks(Schultz et al., 2014; Smith et al., 2009). Further increasing NIC = 4, we observe that the primary visual network (Fig. 3d) is split off from the primary sensory network (Fig. 1a or Fig. 2a).

The 3-way ANOVA modeling of the ICA results at low NIC produced very little statistical contrast. When NIC ≥ 7, the ICA parcellation becomes sufficiently specific and renders significant statistical contrast in the 3-way ANOVA of the ICA results. Figs. 4–6 depict the 3-way ANOVA results of the ICA results at NIC = 10. As shown in Fig. 4 and Table 2, the brain regions with significant group effect in intrinsic functional activity include mainly anterior cingulate, left inferior frontal gyrus and middle/superior temporal gyri. The boxplots of the average z-score values for the ROIs with significant group effect (see Fig. 4) indicate that migraines patients have reduced intrinsic activity in involved functional networks (Fig. 7a and b).

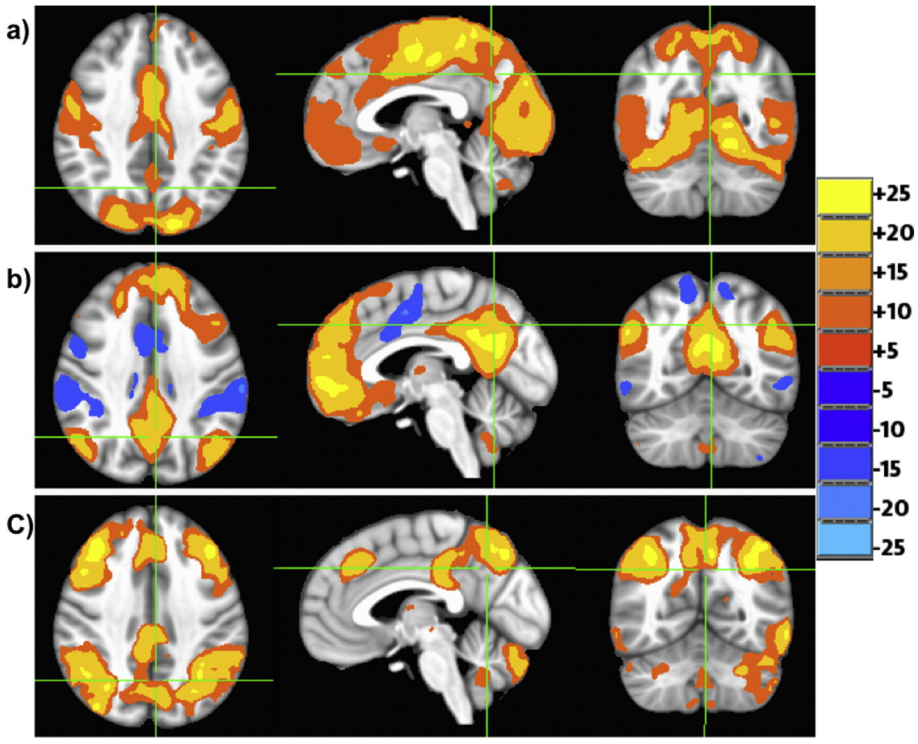

Fig. 2. The cross-sectional displays of the one-sampled t-score maps (t ≥ 4.0 and minimum cluster size of 20) for group ICA result at NIC = 3. Besides the primary sensory network consisting of the somatosensory motor, auditory, and visual systems (a) and the extended default mode network (b) observed at NIC = 2, the symmetrically mirrored left- and right-control RFN (c) is also seen. The color bar indicates the t-score level. (For interpretation of the references to color in this figure legend, the reader is referred to the web version of this article.)

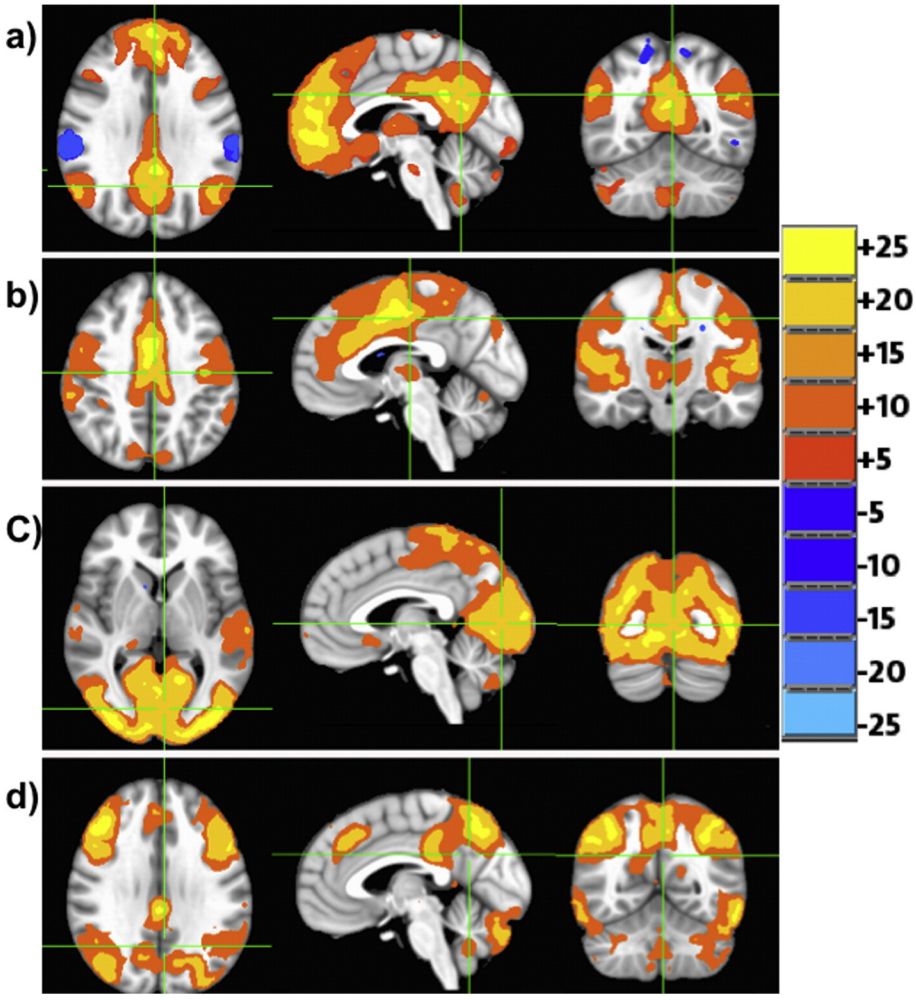

Fig. 3. The cross-sectional displays of the one-sampled t-score maps (t ≥ 4.0 and minimum cluster size of 20) for group ICA result at NIC = 4. Compared with the over determined ICs observed at NIC = 3, the primary sensory network is split into two separate ICs. (a) The default mode network. (b) The somatosensory motor network. (c) The visual system. (d) The symmetrically mirrored left- and right-control RFN. The color bar indicates the t-score level. (For interpretation of the references to color in this figure legend, the reader is referred to the web version of this article.)

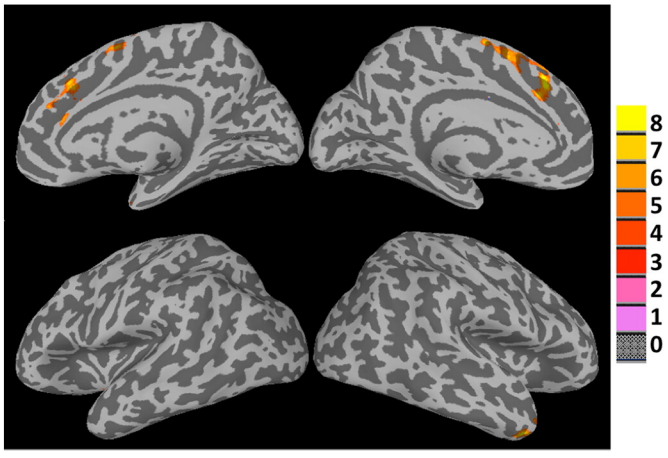

Fig. 4. Brain regions with significant subject group effect (migraine patients versus healthy controls) in intrinsic functional activity at NIC = 10. The statistical significance was assessed with the 3-way ANOVA (model type = 5) at voxel-wise F-score threshold F ≥ 7.385 (numerator DF = 1, denominator DF = 36, uncorrected p ≤ 0.01) and a minimum cluster size of 20 contiguous voxels. The color bar indicates the F-score level. (For interpretation of the references to color in this figure legend, the reader is referred to the web version of this article.)

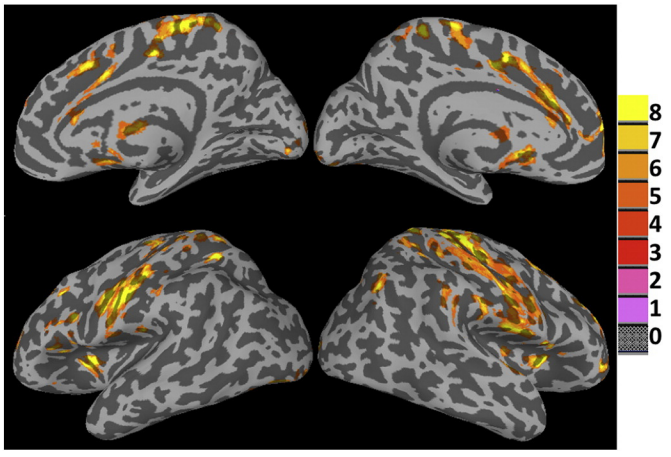

Fig. 5. Brain regions with significant KOS treatment effect on the instinct functional activity at NIC = 10. The statistical significance was assessed with the 3-way ANOVA (model type = 5) at voxel-wise F-score threshold F ≥ 4.373 (numerator DF = 3, denominator DF = 36, uncorrected p ≤ 0.01) and a minimum cluster size of 20 contiguous voxels. The color bar indicates the F-score level. (For interpretation of the references to color in this figure legend, the reader is referred to the web version of this article.)

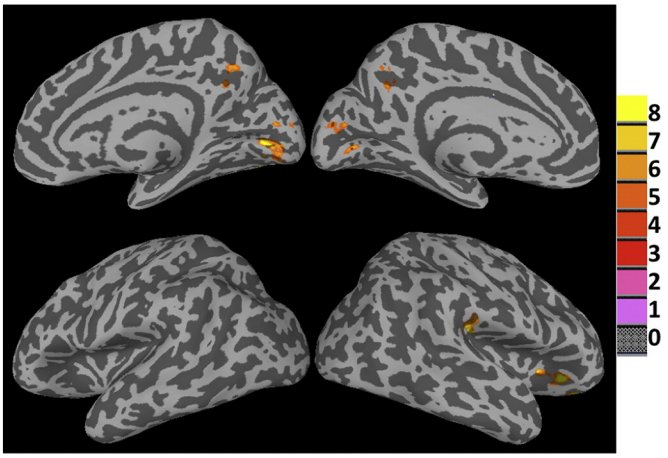

Fig. 6. Brain regions with significant interaction effect between the two main fixed factors. That is, the brain regions where the KOS treatment resulted in significantly difference in the intrinsic functional activity (at NIC = 10) between migraine patients and normal controls. The statistical significance was assessed with the 3-way ANOVA (model type = 5) at voxel-wise F-score threshold $F \geq 4.373$ (numerator DF = 3, denominator DF = 36, $p \leq 0.01$ uncorrected) and a minimum cluster size of 20 contiguous voxels. The color bar indicates the F-score level. (For interpretation of the references to color in this figure legend, the reader is referred to the web version of this article.)

As shown in Fig. 5 and Table 2, broad regions in the limbic and primary sensory systems depicted statistically significant KOS treatment effect on the intrinsic functional activity. The involved brain regions in the limbic system included anterior cingulate, anterior insula cortex, inferior frontal gyrus, thalamus and hypothalamus. These brain areas are important components of the cerebral central control network for the autonomic nervous system. Boxplots of the average z-scores for the involved ROIs are shown in Fig. 7c and d. It is clear that KOS treatment resulted in up-regulated intrinsic functional activity during the treatment in a large number of brain regions of the limbic and primary sensory systems. This trend of change with the KOS procedure is quite similar for both migraine and control participants. However, there are a few more specific regions (see Figs. 6, 7e and f) exhibited opposite trends between the migraine and control groups. The involved brain regions included dorsal posterior insula, lingual gyrus, precuneus and inferior frontal gyrus.

The boxplots in Fig. 7 are the average ROI results of all CA coefficients in 10 networks. To study the specific change in the dorsal posterior insula and inferior frontal gyrus we used also more direct ROI analysis of the CCI and CSI metrics. As shown in Fig. 8, at baseline 1, the CCI values for these brain regions were about the same for both migraine patients and controls, but the CSI values for the migraine patients were about ~7% lower. The probe insertion and the actual KOS treatment reduced CCI by half and CSI by 10%in the normal controls. These changes in CCI and CSI were almost fully recovered for the normal controls after the treatment in baseline 2. However, tor the migraine patients the KOS treatment induced increases in both CCI and CSI. The CCI restored back to the baseline level but the enhanced CSI remained after the treatment. Therefore, the net result of KOS treatment was the up-regulation of CSI in the migraine patients to the level closer to that for the normal controls.

NIC affects the ICA outputs and, therefore, the ANOVA results derived from it, as illustrated by the supplementary materials for NIC = 11 (see Figs. S1–S4). The outcomes from 3-way ANOVA modeling of the ICA results for NIC = 2–19 demonstrate that some of the involved brain regions displayed relatively stable ANOVA statistical contrast irrespective of the input NIC parameter, once NIC ≥ 7. Further details on this can be found in the supplementary materials below.

4. Discussion

4.1. Important findings of the study

Major novel findings of the study are the following: 1) ICA result is directly influenced by the input parameter NIC and NIC has to be sufficiently high to extract functionally specific connectivity networks for further interrogation of clinically relevant questions; 2) migraine patients have altered intrinsic functional activity in anterior cingulate, inferior frontal gyrus, insular cortex and middle/superior temporal gyri; 3) KOS treatment in the nasal cavity can effectively relieve acute migraine symptoms and reduce attack frequency; 4) KOS treatment results in up-regulated intrinsic functional activity in a number of broad brain regions of the limbic and somatosensory systems. However, for migraine patients, the pain relief by the KOS treatment was accompanied with up regulating of intrinsic functional activity in the inferior frontal gyrus and dorsal posterior insula. A recent fMRI study based on ASL technique has also shown that there is a significant coupling between the regional cerebral blood flow in the dorsal posterior insula

Table 2
List of brain regions with significant statistical contrast (FWER $p \leq 0.05$) as identified by voxel-wise 3-way ANOVA modeling of the ICA results with NIC = 10. X, Y, and Z represent the focal locations of ROIs in the standard MNI coordinates. The referred voxel size is 4 mm isotropic.

Statistical contrast	ROI	Volume (voxel)	X (mm)	Y (mm)	Z (mm)	LL/R	Location label
Group	1	110	0.0	−28.0	+34.0	B	Anterior cingulate
	2	49	+16.0	−9.0	−17.0	L	Inferior frontal gyrus
	3	31	−49.0	−1.0	−33.0	R	Middle/superior temporal gyri
Treatment	4	508	+52.0	+12.0	+32.0	L	Pre–postcentral gyrus
	5	411	−60.0	+14.0	+35.0	R	Pre–postcentral gyrus
	6	126	0.0	−13.0	+37.0	B	Anterior cingulate
	7	93	+37.0	−12.0	+5.0	L	Insula, inferior frontal gyrus
	8	81	−38.0	−14.0	+2.0	R	Insula, inferior frontal gyrus
	9	68	−52.0	−8.0	−16.0	R	Superior temporal gyrus
	10	48	−33.0	−48.0	+26.0	R	Middle prefrontal gyrus
	11	31	−31.0	−22.0	+50.0	R	Middle prefrontal gyrus
	12	48	+32.0	−45.0	+16.0	L	Middle prefrontal gyrus
	13	20	+41.0	−28.0	+41.0	L	Middle prefrontal gyrus
	14	32	0.0	+5.0	+9.0	B	Thalamus
	15	23	0.0	−1.0	−14.0	B	Hypothalamus
	16	34	−19.0	+96.0	+7.0	R	Cuneus
	17	51	32.0	+80.0	−11.0	L	Lingual gyrus
	18	22	−38.0	+75.0	+43.0	R	Superior parietal gyrus
Interaction	19	55	−15.0	+79.0	−4.0	R	Lingual gyrus
	20	24	−11.0	+56.0	+31.0	R	Dorsal posterior insula
	21	21	−40.0	−31.0	−9.0	R	Precuneus
	22	20	−44.0	+28.0	+19.0	R	Inferior frontal gyrus

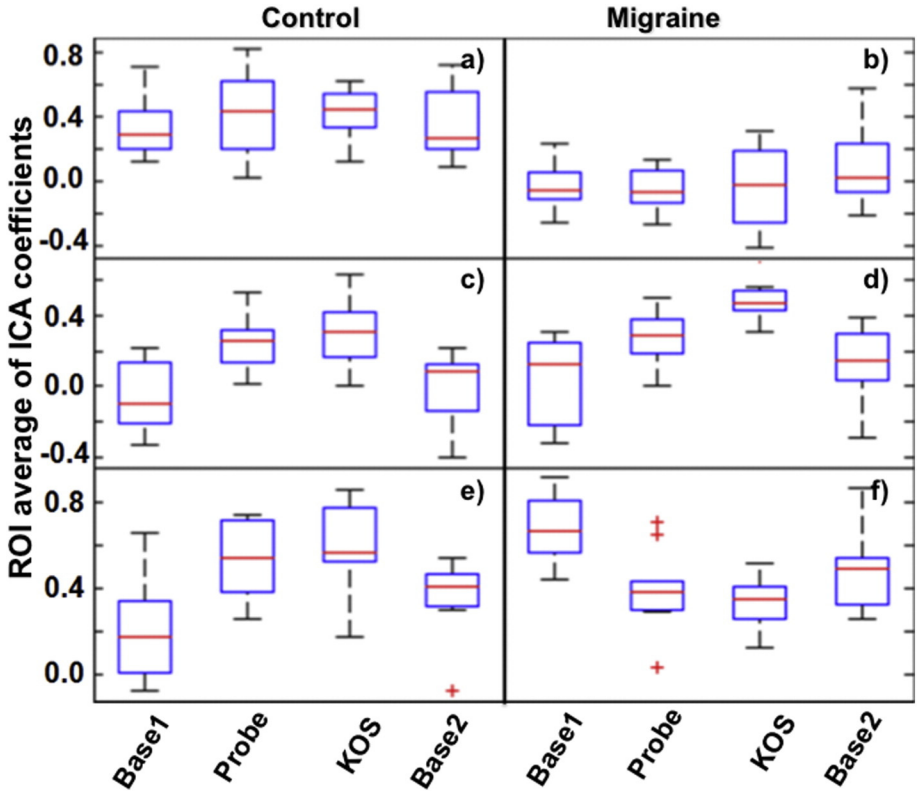

Fig. 7. The ROI average of the IC coefficients for brain regions with significant statistical contrasts (FWER, $p \leq 0.05$) as detected by 3-way ANOVA modeling of the group ICA results at NIC = 10. The group effect between normal controls (a) and migraine patients (b), KOS treatment effect (c and d), and interaction effect between the two main fixed factors (e and f) are displayed.

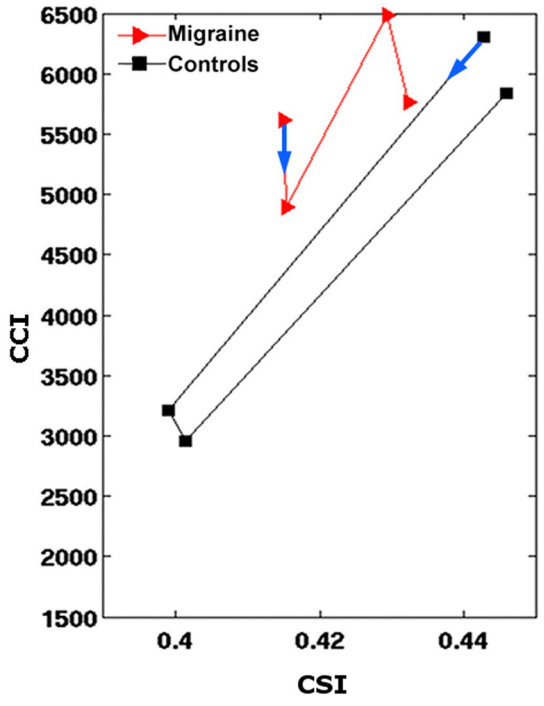

Fig. 8. The ROI average values of CCi are plotted against CSI for the dorsal posterior insula and inferior frontal gyrus where exhibited significant statistical (FWER, $p \leq 0.05$) interaction between the two main fixed factors (subject group and KOS treatment) as detected by the 3-way ANOVA modeling of the resting-state functional connectivity data. The blue arrows indicate the start points of the experimental procedures and the 4 points in each curve represent the measurements conducted at baseline 1, probe insertion, KOS treatment, and baseline 2, respectively. The lines between the data points are connected to guide the eyes.

and the intensity of experienced tonic pain and it has been proposed that dorsal posterior insula is a specific brain region associated with painful experience and a potential therapeutic target (Segerdahl et al., 2015).

KOS of the nasal mucosa with low frequency mechanical vibrations was initially developed to provide an alternative therapy for non-allergic rhinitis (Juto and Axelsson, 2014). Completed single- and multi-site RCT studies (ClinicalTrials.gov Identifier: NCT01844336) have demonstrated that a single KOS treatment has significant impact on reducing the nasal symptoms of persistent rhinitis (Juto and Axelsson, 2014). The effect was most pronounced in the days immediately following treatment but was still present two weeks post-treatment. More recently, an exploratory trials study to test the efficacy of KOS treatment on acute migraine patients demonstrated that this treatment has a surprisingly fast-acting remedy for acute migraine pain (Juto and Hallin, 2015). Results from the present study confirm that KOS is indeed an effective and safe treatment for acute migraine (Juto and Hallin, 2015; Li et al., 2014, 2015b). Comparing with existing treatments for migraine, KOS therapy has the following benefits: 1) easy to administer; 2) well tolerated by the patients; 3) no involvement of pharmaceuticals; 4) very few and mild side effects. KOS in the nasal cavity has the potential to offer a viable alternative both for acute symptom relief and long-term prevention.

4.2. Underlying neurophysiological mechanisms for KOS treatment of migraine

The mechanisms of KOS treatment have not been fully understood. Besides the altered intrinsic functional activities observed in the present study, the measurements of heart rate variability (HRV) during the KOS treatments of migraine patients (not shown) indicate also active responses in the ANS, particularly in the parasympathetic tone. It appears that the intervention has a positive impact on the functioning of ANS

possibly by restoring homeostasis in the basal parts of the brain and the hypothalamic area, which are responsible for short-term ANS control. The observed changes in intrinsic functional activity in the limbic system in association with the pain relief by KOS treatment reflect more likely the intermediate and longer-term adjustment of ANS by the central nervous control network.

It has been previously demonstrated that electrical stimulation of the PPG can mitigate severe symptoms in primary headaches (Altinay et al., 2015; Palmisani et al., 2013), implying that the stimulation of PPG by the KOS treatment in the nasal cavity is at least partly responsible for the migraine pain relief through the trigeminal parasympathetic reflex. Recent studies provided new anatomic insight into the PPG innervation of the posterolateral nasal mucosa (Bleier and Schlosser, 2011; Li et al., 2015a; Li et al., 2010). Neurons project from the PPG via multiple individual postganglionic rami to supply the nasal mucosa (Bleier and Schlosser, 2011) and PPG is directly connected to hypothalamus through the parasympathetic fibers from the superior salivatory nucleus (Li et al., 2015a; Li et al., 2010). Growing evidence from functional imaging studies indicates that hypothalamus plays a very important role in the pathogenesis of migraine attacks (Arkink et al., 2012; Charles, 2013; Kato et al., 2010; Kroger and May, 2014; Lipton et al., 2014; Maniyar et al., 2014; Maniyar et al., 2015; May, 2010, 2013; Montagna et al., 2010; Morelli et al., 2013; Moulton et al., 2014; Robert et al., 2013; Sahler, 2013; Schwedt et al., 2015; Seifert et al., 2012; Zielman et al., 2014). Migraine patients seem to have a normally regulated ANS when symptom free between attacks. However, during headache attacks they suffer typically the symptoms of an unbalanced ANS.

Preliminary studies of patients with chronic inflammatory disorders, such as, granulomatosis with polyangiitis and dialysis patients with kidney failure (ISRCTN49663124 DOI 10.1186/ISRCTN49663124) indicate that KOS in the nasal cavity may have promising anti-inflammatory efficacy. This suggests that KOS treatment may has similar impact as the electric stimulation of vagus nerve (Andersson and Tracey, 2012; Bonaz et al., 2013; Huston, 2012) and might also involve the activation of the cholinergic anti-inflammatory pathway (Tracey, 2002, 2009) through the interconnections between cranial nerves in the nasal cavity. We will investigate this aspect further in the near future.

4.3. The main strength and weakness of the study

The strengths of this study include the following: 1) KOS treatment of on-going acute migraine was investigated inside MRI scanner with simultaneous BOLD fMRI recordings; 2) non-invasive KOS treatment was also conducted in normal volunteers with the identical procedure and direct comparison between migraine patients and normal controls can be performed; 3) voxel-wise data-driven analysis based on 3-way ANOVA modeling of the ICA results was conducted systematically for a wide range of NIC = 2–19.

The main weaknesses of the study are the following: 1) The data analysis based on ICA does not provide quantitative metrics for neurophysiology activity, which renders the results difficult to interpret and dependent on the input value for NIC. Therefore, it is necessary to provide complementary results based on ROI analysis of functional connectivity metrics. 2) There was no data available for migraine patients under migraine-free period. A crossover study design with the patients as their own controls has definitely its advantage for identifying possible prophylactic effect of KOS treatment. 3) Simultaneous monitoring of HRV during fMRI measurements would be very useful for more detailed interpretation of the neurophysiological mechanisms underlying KOS treatment of acute migraine. However, the interfering artifacts caused by the pulsing magnetic field gradients currently limit simultaneous electrocardiography recording during fMRI.

5. Conclusion

The result of this study confirms that KOS treatment is effective both in relieving acute migraine headache and reducing attack frequency. Migraine is associated with aberrant intrinsic functional activity in the limbic and primary sensory systems. KOS in the nasal cavity can regulate the intrinsic functional connectivity in the limbic system and restore favorably the neurophysiological homeostasis in the ANS. The preliminary findings from this pilot study with limited number of participants should be further verified with larger studies in the future.

Supplementary data to this article can be found online at http://dx.doi.org/10.1016/j.nicl.2016.08.014.

Acknowledgements

This study was supported by research grants from the Swedish Research Council and ALF Medicine in Stockholm Province. The authors also want to acknowledge the support from Karolinska Institute and Karolinska University Hospital.

References

Alstadhaug, K.B., 2014. Histamine in migraine and brain. Headache 54, 246–259.
Altinay, M., Estemalik, E., Malone Jr., D.A., 2015. A comprehensive review of the use of deep brain stimulation (DBS) in treatment of psychiatric and headache disorders. Headache 55, 345–350.
Andersson, U., Tracey, K.J., 2012. A new approach to rheumatoid arthritis: treating inflammation with computerized nerve stimulation. Cerebrum 2012, 3.
Arkink, E.B., Bleeker, E.J., Schmitz, N., Schoonman, G.G., Wu, O., Ferrari, M.D., van Buchem, M.A., van Osch, M.J., Kruit, M.C., 2012. Cerebral perfusion changes in migraineurs: a voxelwise comparison of interictal dynamic susceptibility contrast MRI measurements. Cephalalgia 32, 279–288.
Bahra, A., Matharu, M.S., Buchel, C., Frackowiak, R.S., Goadsby, P.J., 2001. Brainstem activation specific to migraine headache. Lancet 357, 1016–1017.
Bleier, B.S., Schlosser, R.J., 2011. Endoscopic anatomy of the postganglionic pterygopalatine innervation of the posterolateral nasal mucosa. Int. Forum Allergy Rhinol. 1, 113–117.
Bonaz, B., Picq, C., Sinniger, V., Mayol, J.F., Clarencon, D., 2013. Vagus nerve stimulation: from epilepsy to the cholinergic anti-inflammatory pathway. Neurogastroenterology 25, 208–221.
Charles, A., 2013. The evolution of a migraine attack - a review of recent evidence. Headache 53, 413–419.
Danese, E., Montagnana, M., Lippi, G., 2014. Platelets and migraine. Thromb. Res. 134, 17–22.
Dussor, G., 2014. Serotonin, 5HT1 agonists, and migraine: new data, but old questions still not answered. Curr. Opin. Support Palliat. Care 8, 137–142.
Ebinger, F., Kruse, M., Just, U., Rating, D., 2006. Cardiorespiratory regulation in migraine. Results in children and adolescents and review of the literature. Cephalalgia 26, 295–309.
Friberg, L., Olesen, J., Lassen, N.A., Olsen, T.S., Karle, A., 1994. Cerebral oxygen extraction, oxygen consumption, and regional cerebral blood flow during the aura phase of migraine. Stroke 25, 974–979.
Friedman, D.I., De ver Dye, T., 2009. Migraine and the environment. Headache 49, 941–952.
Gawel, M.J., Rose, F.C., 1982. Platelet function in migraineurs. Adv. Neurol. 33, 237–242.
Geraud, G., Donnet, A., 2013. Migraine and hypothalamus. Rev. Neurol. (Paris) 169, 372–379.
Geraud, G., Denuelle, M., Fabre, N., Payoux, P., Chollet, F., 2005. Positron emission tomographic studies of migraine. Rev. Neurol. 161, 666–670.
Hanington, E., 1989. Migraine: the platelet hypothesis after 10 years. Biomed. Pharmacother. 43, 719–726.
Hoffmann, J., Goadsby, P.J., 2014. Emerging targets in migraine. CNS Drugs 28, 11–17.
Huston, J.M., 2012. The vagus nerve and the inflammatory reflex: wandering on a new treatment paradigm for systemic inflammation and sepsis. Surg. Infect. 13, 187–193.
Iacovelli, E., Coppola, G., Tinelli, E., Pierelli, F., Bianco, F., 2012. Neuroimaging in cluster headache and other trigeminal autonomic cephalalgias. J. Headache Pain 13, 11–20.
Juto, J.E., Axelsson, M., 2014. Kinetic oscillation stimulation as treatment of non-allergic rhinitis: an RCT study. Acta Otolaryngol. 134, 506–512.
Juto, J.E., Hallin, R., 2015. Kinetic oscillation stimulation as treatment of acute migraine. A randomized, controlled pilot study. Headache 55, 11.
Kato, Y., Araki, N., Matsuda, H., Ito, Y., Suzuki, C., 2010. Arterial spin-labeled MRI study of migraine attacks treated with rizatriptan. J. Headache Pain 11, 255–258.
Kroger, I.L., May, A., 2014. Central effects of acetylsalicylic acid on trigeminal-nociceptive stimuli. J. Headache Pain 15, 59.
Kroger, I.L., May, A., 2015. Triptan-induced disruption of trigemino-cortical connectivity. Neurology 84, 2124–2131.
Lacombe, P., Sercombe, R., Correze, J.L., Springhetti, V., Seylaz, J., 1992. Spreading depression induces prolonged reduction of cortical blood flow reactivity in the rat. Exp. Neurol. 117, 278–286.

Li, C., Fitzgerald, M.E., Ledoux, M.S., Gong, S., Ryan, P., Del Mar, N., Reiner, A., 2010. Projections from the hypothalamic paraventricular nucleus and the nucleus of the solitary tract to prechoroidal neurons in the superior salivatory nucleus: pathways controlling rodent choroidal blood flow. Brain Res. 1358, 123–139.
Li, T.Q., Yang, Y., Hallin, R., Juto, J.E., 2014. Novel intervention for acute migraine headache investigated by BOLD fMRI. Proc. ISMRM 2014, 2016.
Li, C., Fitzgerald, M.E., Del Mar, N., Cuthbertson-Coates, S., LeDoux, M.S., Gong, S., Ryan, J.P., Reiner, A., 2015a. The identification and neurochemical characterization of central neurons that target parasympathetic preganglionic neurons involved in the regulation of choroidal blood flow in the rat eye using pseudorabies virus, immunolabeling and conventional pathway tracing methods. Front. Neuroanat. 9, 65.
Li, T.Q., Yang, Y., Hallin, R., Juto, J.E., 2015b. Kinetic oscillatory stimulation (KOS) in the nasal cavity studied by resting-state fMRI. Proc. ISMRM 2015, 6193.
Lipton, R.B., Buse, D.C., Hall, C.B., Tennen, H., Defreitas, T.A., Borkowski, T.M., Grosberg, B.M., Haut, S.R., 2014. Reduction in perceived stress as a migraine trigger: testing the "let-down headache" hypothesis. Neurology 82, 1395–1401.
Lodi, R., Pierangeli, G., Tonon, C., Cevoli, S., Testa, C., Bivona, G., Magnifico, F., Cortelli, P., Montagna, P., Barbiroli, B., 2006. Study of hypothalamic metabolism in cluster headache by proton MR spectroscopy. Neurology 66, 1264–1266.
Maniyar, F.H., Sprenger, T., Monteith, T., Schankin, C., Goadsby, P.J., 2014. Brain activations in the premonitory phase of nitroglycerin-triggered migraine attacks. Brain 137, 232–241.
Maniyar, F.H., Sprenger, T., Monteith, T., Schankin, C.J., Goadsby, P.J., 2015. The premonitory phase of migraine—what can we learn from it? Headache 55, 609–620.
May, A., 2010. The window into headache research: what have we learned from functional and structural neuroimaging. Schmerz 24, 130–136.
May, A., 2013. Pearls and pitfalls: neuroimaging in headache. Cephalalgia 33, 554–565.
Melek, I.M., Seyfeli, E., Duru, M., Duman, T., Akgul, F., Yalcin, F., 2007. Autonomic dysfunction and cardiac repolarization abnormalities in patients with migraine attacks. Med. Sci. Monit. 13, RA47–RA49.
Montagna, P., Pierangeli, G., Cortelli, P., 2010. The primary headaches as a reflection of genetic Darwinian adaptive behavioral responses. Headache 50, 273–289.
Morelli, N., Rota, E., Gori, S., Guidetti, D., Michieletti, E., De Simone, R., Di Salle, F., 2013. Brainstem activation in cluster headache: an adaptive behavioural response? Cephalalgia 33, 416–420.
Moulton, E.A., Becerra, L., Johnson, A., Burstein, R., Borsook, D., 2014. Altered hypothalamic functional connectivity with autonomic circuits and the locus coeruleus in migraine. PLoS One 9, e95508.
Nordin, L.E., Moller, M.C., Julin, P., Bartfai, A., Hashim, F., Li, T.Q., 2016. Post mTBI fatigue is associated with abnormal brain functional connectivity. Sci. Rep. 6, 21183.
Palmisani, S., Al-Kaisy, A., Arcioni, R., Smith, T., Negro, A., Lambru, G., Bandikatla, V., Carson, E., Martelletti, P., 2013. A six year retrospective review of occipital nerve stimulation practice—controversies and challenges of an emerging technique for treating refractory headache syndromes. J. Headache Pain 14, 67.
Pollock, J.M., Deibler, A.R., Burdette, J.H., Kraft, R.A., Tan, H., Evans, A.B., Maldjian, J.A., 2008. Migraine associated cerebral hyperperfusion with arterial spin-labeled MR imaging. AJNR Am. J. Neuroradiol. 29, 1494–1497.
Raddant, A.C., Russo, A.F., 2014. Reactive oxygen species induce procalcitonin expression in trigeminal ganglia glia. Headache 54, 472–484.
Robert, C., Bourgeais, L., Arreto, C.D., Condes-Lara, M., Noseda, R., Jay, T., Villanueva, L., 2013. Paraventricular hypothalamic regulation of trigeminovascular mechanisms involved in headaches. J. Neurosci. 33, 8827–8840.
Sahler, K., 2013. Hemicrania continua: functional imaging and clinical features with diagnostic implications. Headache 53, 871–872.
Scher, A.I., Bigal, M.E., Lipton, R.B., 2005. Comorbidity of migraine. Curr. Opin. Neurol. 18, 305–310.
Schultz, A.P., Chhatwal, J.P., Huijbers, W., Hedden, T., van Dijk, K.R., McLaren, D.G., Ward, A.M., Wigman, S., Sperling, R.A., 2014. Template based rotation: a method for functional connectivity analysis with a priori templates. NeuroImage 102 (Pt 2), 620–636.
Schwedt, T.J., Chiang, C.C., Chong, C.D., Dodick, D.W., 2015. Functional MRI of migraine. Lancet 14, 81–91.
Segerdahl, A.R., Mezue, M., Okell, T.W., Farrar, J.T., Tracey, I., 2015. The dorsal posterior insula subserves a fundamental role in human pain. Nat. Neurosci. 18, 499–500.
Seifert, C.L., Magon, S., Staehle, K., Zimmer, C., Foerschler, A., Radue, E.W., Pfaffenrath, V., Tolle, T.R., Sprenger, T., 2012. A case-control study on cortical thickness in episodic cluster headache. Headache 52, 1362–1368.
Smith, S.M., Fox, P.T., Miller, K.L., Glahn, D.C., Fox, P.M., Mackay, C.E., Filippini, N., Watkins, K.E., Toro, R., Laird, A.R., Beckmann, C.F., 2009. Correspondence of the brain's functional architecture during activation and rest. Proc. Natl. Acad. Sci. U. S. A. 106, 13040–13045.
Tajti, J., Szok, D., Majlath, Z., Tuka, B., Csati, A., Vecsei, L., 2015. Migraine and neuropeptides. Neuropeptides 52, 19–30.
Tracey, K.J., 2002. The inflammatory reflex. Nature 420, 853–859.
Tracey, K.J., 2009. Reflex control of immunity. Nat. Rev. Immunol. 9, 418–428.
Vollbracht, S., Rapoport, A.M., 2014. New treatments for headache. Neurol. Sci. 35 (Suppl 1), 89–97.
Wang, Y., Li, T.Q., 2013. Analysis of whole-brain resting-state FMRI data using hierarchical clustering approach. PLoS One 8, e76315.
Wang, Y., Li, T.Q., 2015. Dimensionality of ICA in resting-state fMRI investigated by feature optimized classification of independent components with SVM. Front. Hum. Neurosci. 9, 259.
Wang, S.J., Lirng, J.F., Fuh, J.L., Chen, J.J., 2006. Reduction in hypothalamic 1H-MRS metabolite ratios in patients with cluster headache. J. Neurol. Neurosurg. Psychiatry 77, 622–625.
Zielman, R., Teeuwisse, W.M., Bakels, F., Van der Grond, J., Webb, A., van Buchem, M.A., Ferrari, M.D., Kruit, M.C., Terwindt, G.M., 2014. Biochemical changes in the brain of hemiplegic migraine patients measured with 7 tesla 1H-MRS. Cephalalgia 34, 959–967.